Check for updates

Habitat changes and catch rate variability for greater amberjack in the Taiwan Strait: The effects of El Niño–southern oscillation events

Mubarak Mammel[1], Ming-An Lee[1,2,3]*, Muhamad Naimullah[1], Cheng-Hsin Liao[1,2], Yi-Chen Wang[1,3] and Bambang Semedi[4]

[1]Department of Environmental Biology and Fisheries Science, National Taiwan Ocean University, Keelung, Taiwan, [2]Doctoral Degree Program in Ocean Resource and Environmental Changes, National Taiwan Ocean University, Keelung, Taiwan, [3]Center of Excellence for Oceans, National Taiwan Ocean University, Keelung, Taiwan, [4]Fisheries and Marine Science Faculty, Brawijaya University, Malang, East Java, Indonesia

El Niño–Southern Oscillation (ENSO) is a crucial oceanographic phenomenon that leads to interannual fluctuations in the climate and ecosystem productivity of tropical and subtropical areas. These fluctuations affect the suitability of habitats for many commercial fish species. However, detailed information on the effects of this major phenomenon and the resulting environmental changes on the habitat and catch rates of the economically and ecologically crucial species of the greater amberjack (Seriola dumerili) in the Taiwan Strait (TS) is lacking. In this study, we employed a weighted habitat suitability index (HSI) modeling method and used remotely sensed marine environmental data as well as data from recorders in Taiwanese fishing vessels (in 2014−2019) to understand the effects of ENSO events on the habitat suitability and catch rates for greater amberjack in the TS. Analysis of variance revealed that environmental factors substantially influenced greater amberjack habitats and catch rates during ENSO events across seasons. The catch rates were high in spring and summer in the southern and northern TS and in autumn and winter in the southern TS. The catch rates were higher in spring, summer, and autumn (>9.0 kg/h) in El Niño years, and in winter, the catch rates were higher in normal years (>12.0 kg/h) and lower in La Niña years. The predicted HSI for the southern and northern TS revealed that greater amberjack populations were predominantly distributed at 20−24°N and 24−28°N, respectively. Opposite habitat suitability was synchronously found in spring and summer during ENSO events, with higher HSI values recorded in spring in El Niño and normal years and higher HSI values recorded in summer in La Niña years. In winter, the HSI values of the southern and northern TS were higher in El Niño and normal years and substantially lower

in La Niña years. Habitat suitability was extremely low in autumn. These findings imply that ENSO events play a key role in regulating environmental conditions and affect the catch rates and habitat suitability for the greater amberjack in the TS.

Introduction

The greater amberjack (*Seriola dumerili*) are marine pelagic species that can be found all over the world from the temperate to the tropical waters (Taki et al., 2005). The species has commercial and recreational fishing value (Gold and Richardson, 1998) as well as high aquaculture potential (Nakada, 2008). Greater amberjack is the largest pelagic group in the Carangidae family and is an opportunistic predator species that can mainly be observed in areas near reef-associated floating objects, such as drifting seaweed, in the open ocean (Sley et al., 2016; Hasegawa et al., 2020). In the waters of Taiwan, greater amberjack fishery resources have been steadily increasing. The species is notable for its outstanding quality meat, quick growth, substantial commercial value in a vast international market, and global distribution. However, an increase in fishing efforts and landings has led the greater amberjack species to become classified as overfished (Turner et al., 2000). Two subpopulations of the greater amberjack have been identified along the coasts of East Asia in the East China Sea (ECS) and the South China Sea (SCS) in addition to two subpopulations identified off the coast of the United States (Hasegawa et al., 2020). However, the status of the greater amberjack in Taiwanese waters remains unknown, and no strategies to conserve or manage the greater amberjack have been developed. To effectively develop strategies for managing this valuable fishery resource, information on the habitat preferences of and climate-related environmental effects on the fish is required. However, although fish habitat distribution and climate-related environmental effects have been reported to be essential factors affecting fish populations, the data available on the greater amberjack population in the waters of Taiwan are almost entirely based on assessments of age and growth (Hasegawa et al., 2017; Hasegawa et al., 2020), migration, and spawning (Tone et al., 2022).

The Taiwan Strait (TS) is a shallow shelf zone and an important fishing region from the tropical to subtropical in the western Pacific Ocean between Taiwan and China. The TS is also a crucial water pathway that connects the SCS in the south and the ECS in the north, and it transports water and chemical elements along the western coast of Taiwan. The biogeochemical, physical, and ecological dynamics of the TS fluctuate considerably over time and space because of its complicated bottom topography that alternately forces the monsoon and the convergence of numerous current systems (Gong et al., 2003; Naik and Chen, 2008; Tseng

et al., 2020). The TS is approximately 350-km long and 180-km width, having an average depth of 60 m. The TS has greater than 200 m in depth in the southeast (Lan et al., 2009; Naimullah et al., 2020). The three main currents that influence the waters around the TS are the China Coastal, Kuroshio Branch, and SCS currents. A notable topographical feature in the TS is the Chang-Yuen Rise, which stretches westward from the middle of Taiwan's western coast. The Chang-Yuen Rise divides the TS into two basins and creates an ocean circulation barrier, with the China Coastal Water to the north and the SCS Warm Current and Kuroshio Branch Current to the south (Lee et al., 2003). The warm Kuroshio current flows along Taiwan's eastern coast, and a cold dome frequently forms over the continental shelf's northeastern edges (Lan et al., 2020). The Kuroshio Branch Current influences the transportation of greater amberjack fish eggs, larvae, and juveniles (Sassa et al., 2008; Sassa and Tsukamoto, 2010). An important location for the spawning area of the greater amberjack is located near the open water region off the Penghu Islands of Taiwan, in the southern part of the TS (Hasegawa et al., 2020).

To effectively manage marine resources, understanding the distribution patterns of marine species in terms of space and time are crucial. These patterns enable researchers to determine the environmental characteristics that affect how species respond to environmental changes as well as their range and habitat preferences. This information can assist in improving ecosystem management (Saraux et al., 2014), fish stocks and abundance (Azevedo and Silva, 2020), and prey abundance and dispersion (Garrison et al., 2002) and in habitat conservation (Ward et al., 2015) and fishery management (Kai et al., 2017). Satellite-derived environmental variables and temporal and spatial distribution patterns can be utilized to locate and predict potentially suitable fish habitats and distribution (Mansor et al., 2001; Zhang et al., 2017; Lee et al., 2018; Abdul Azeez et al., 2021).

Climate change has led to worldwide biodiversity redistribution (Pecl et al., 2017), with alterations in species distributions occurring faster in marine habitats than in terrestrial systems (Chen et al., 2011; Poloczanska et al., 2013). Diverse groups of marine species have exhibited consistent poleward tendencies in response to climate change (Poloczanska et al., 2013). These tendencies demonstrate the projected and actual effects of climate change on oceanographic variables (Wu et al., 2012). Many researchers have focused on determining the effects of changes in habitat suitability due to climate variability and their interactions with fish

distributions and abundance and catches; these data would be crucial for achieving prudent exploitation of fish resources and sustainable management (Silva et al., 2016; Tanaka and Chen, 2016). The El Niño–Southern Oscillation (ENSO) phenomenon is considered a crucial indicator of large-scale environmental and climatological variability related to climate change, and the phenomenon exerts considerable effects on the distribution and production of fish species in the oceans (Anderson and Rodhouse, 2001). The environmental conditions that occur during the respective oceanic warming and cooling of El Niño and La Niña have both the positive and the negative effects on the abundance index (Tian et al., 2003). The ENSO phenomenon happens in the tropical Pacific Ocean and is an indicator of interannual oscillations. The ENSO phenomenon is caused by changes in surface wind pressure and the sea surface temperature (SST). These changes offer intermediary reasons for climatic variations in El Niño and La Niña years (McPhaden et al., 2006). The SST in the eastern and central tropical Pacific is lower than the average in La Niña years and is higher than the average in El Niño years (Naimullah et al., 2021).

In this study, we used a habitat suitability model for the greater amberjack in the TS that incorporated climate-related oceanographic characteristics to better understand and enable future predictions of the greater amberjack's environmental habitat by using multiple oceanographic predictors. The implications of climate change for the greater amberjack habitats in the waters of Taiwan are unknown. Therefore, examining the causes and effects of climate change on the greater amberjack habitats is crucial. The goal of this research is to build an integrated habitat suitability model to investigate the habitat suitability for the greater amberjack in the TS and to quantify climate-driven shifts in different types of El Niño and La Niña episodes. In response to the effects of climate change, the present study also provides suitable fishery resource management and conversation measures based on an analysis of synchronous changes that occur during different ENSO episodes and thus offers science-based suggestions for the sustainable management and responsible use of the habitat patterns of the greater amberjack in the TS.

Materials and methods

Greater amberjack fishery data

Daily spatial high resolution fisheries data of the greater amberjack from 2014 to 2019 were collected using voyage data recorders from the Taiwanese fishing vessels (5–200 MT) that are equipped with an angling gear and operate in the TS. The fishing data included latitude and longitude, fishing date, operating hours, total catch (kg), and targeted species. These data obtained 0.1° spatial grids were used to collect data from daily fishing locations. To adjust for fishing effort, the monthly catch rates were determined (Equation (1)) by dividing the total weight of the greater amberjack caught by all the fishing vessels over the course of a month by the total operating hours at all the fishing locations during that month. The monthly catch rates for each 0.1° grid within the study area

were used in the following formula, where i is the latitude, and j is the longitude for each 0.1° spatial grid. We used MATLAB software to create catch rate distribution maps for the greater amberjack.

$$\text{Catch rate}_{ij} = \frac{\sum \text{Catch for all the vessels (kg)}_{ij}}{\sum \text{Operating time for all the vessels (hour)}_{ij}} \quad (1)$$

Satellite-derived marine environmental data

The monthly SST, sea surface salinity (SSS), sea surface height (SSH), mixed layer depth (MLD), and eddy kinetic energy (EKE) marine environmental data were obtained from the Copernicus Marine Environment Monitoring Service (https://marine.copernicus.eu) at a horizontal resolution of 1/12°. The monthly chlorophyll-a concentration (Chl-a) data were extracted from the National Aeronautics and Space Administration's (NASA) Aqua satellite (oceancolor.gsfc.nasa.gov), which has a sensor for measuring Chl-a in oceans. Monthly temporal and spatial resolution of 4.6 km (at the equator) were found in the level 3 data map image of the Chl-a data. All remotely sensed marine environmental data from 2014 to 2019 were downloaded and were then resampled, with monthly means derived on a 0.1° spatial grid, which corresponded to the spatial grid employed for the fishery data. To construct Hövmöller plots of spatiotemporal variations in oceanographic conditions of the six environmental variables were extracted using MATLAB on a monthly timescale throughout the regions covering the TS (20–29°N). The monthly average values of all the environmental variables included in the study from 2014 to 2019 in the TS were utilized to produce the monthly average time-series trends analysis. Before statistical models were used, the relationships between the environmental data were examined to calculate the correlation coefficients between the variables. When all the environmental variables were tested for intercorrelations, low correlation coefficients ($r^2 < 0.25$) were found.

Climatic Niño index

To calculate the tropical climatic index, we were considered the Oceanic Niño Index (ONI), which is an ENSO-associated index, and investigated the association between the ONI and the mean catch rates of the greater amberjack. The ONI was used to define ENSO events, which were considered running 3-month mean SST anomalies between 5°N–5°S and 120°–170°W in the Niño 3.4 region. El Niño and La Niña episodes were outlined as five consecutive and overlapping 3-month period intervals in which the ONI was above +0.5°C or below −0.5°C, respectively. During the study years, the ONI's positive and negative values alternated, indicating considerable interannual variations in oceanographic conditions. An ONI range of ±0.5°C was described as a normal year. The ONI values were obtained from the National Oceanic and Atmospheric Administration's (NOAA) Climate Prediction Center and were accessed from the center's website (https://origin.cpc.ncep.noaa.gov/products/analysis_monitoring/ensostuff/ONI_v5.php).

Statistical analysis

One-way analysis of variance (ANOVA) were utilized to analyze the associations between the greater amberjack catch rates and environmental variables during ENSO events based on the location in the TS at which the fishery data were obtained from 2014 to 2019. Tukey's tests were used to perform pairwise *post hoc* comparisons. We checked and confirmed that the necessary presumptions that the variance was homogeneous, the errors had a normal distribution, and error independence of the one-way ANOVA were met.

Partial least squares regression method

The partial least squares regression (PLSR) approach can be used to compress data by reducing a large number of collinear spectral variables into a small number of set especially when the variables are multicollinearity. This strategy is progression from multiple regression analysis, which can be used to determine the influence of several predictors in linear combinations of one or more response variables (Carrascal et al., 2009). In a previous study, the predictor variables of (catch rates >60%) with latent structure and response variables (six environmental factors) was accounted for by using PLSR, which can be used to select the model with the best predictor variables that most favorably reflect the changes in response variables (Wold et al., 2001). In the present study, to evaluate the predictors' relative importance in the overall model, we determined the PLSR for the variable influence on projection (VIP) scores. Based on VIP scores, the relative weighting was proportionately determined. In the present study, for developing the HSI model for the greater amberjack, we used six weights based on VIP scores.

Development of the habitat suitability index model

The habitat suitability index (HSI) model has been widely used to evaluate the spatiotemporal distribution patterns of potential habitats for marine species (Feng et al., 2022). Many studies have used multiple marine environmental factors to develop HSI models for a single species (Yen et al., 2012; Chang et al., 2019; Lee et al., 2020; Vayghan et al., 2020). The HSI model has become an increasingly crucial ecological tool for identifying species responses to climate-related environmental variability to enable the conservation, management, and restoration of valuable marine resources. HSI models are mainly based on a suitability index (SI), and they are habitat quality indicators that determine the associations between one or more key environmental factors and the abundance of key species or the occurrence of a specific species (Yu and Chen, 2020). An HSI value ranging between 0 and 1 indicates that a habitat is likely suitable for a species, with 0

indicating that a habitat is completely unsuitable and 1 indicating that a habitat is completely suitable. The associations between the catch rates for the greater amberjack and all the environmental factor were shown as curves representing the SI values, with a catch rate of >60% being considered a high catch. The following formula (Equation (2)) was used to calculate the SI values:

$$SI_{ij} = \frac{\text{Catch rates}_{ij}}{\text{Max(Catch rates}_{ij})} \qquad (2)$$

where catch rates$_{ij}$ represents the total fishing efforts over the ith interval of the range of the environmental factors j, and max(catch rates$_{ij}$) represents the maximum total fishing efforts. The following formula (Equation (3) to (8)) can be used to determine the associations between the SI and environmental factors for the greater amberjack, where α and β are constants, and the environmental factors included in this research.

$$SI_{SST} = \text{Exp}[\alpha(SST - \beta)^2] \qquad (3)$$

$$SI_{SSS} = \text{Exp}[\alpha(SSS - \beta)^2] \qquad (4)$$

$$SI_{SSH} = \text{Exp}[\alpha(SSH - \beta)^2] \qquad (5)$$

$$SI_{Chl-a} = \text{Exp}[\alpha((Chl - a) - \beta)^2] \qquad (6)$$

$$SI_{MLD} = \text{Exp}[\alpha(MLD - \beta)^2] \qquad (7)$$

$$SI_{EKE} = \text{Exp}[\alpha(EKE - \beta)^2] \qquad (8)$$

Several models, such as the geometric mean model, the continuous product model, the minimum model, and the arithmetic mean model (AMM), can be combined with SI models to form integrated HSI models (Lee et al., 2018). However, numerous studies have reported that the AMM is the most favorable for HSI models, and that it has led to optimal results for several fish species (Yen et al., 2012; Li et al., 2014; Lee et al., 2020). Therefore, the AMM was used in the present study; the setting weights of different environmental factors were reported Naimullah et al. (2021) to substantially impact HSI modeling. The weighted HSI AMM was estimated (Equation (9)) using the following formula:

$$HSI_{AMM} = \frac{1}{\sum_{i=1}^{n} w_i} \sum_{i=1}^{n} (SI_i \times w_i) \qquad (9)$$

where SI_i is the SI value for all the environmental factor i; w_i is the weight of each environmental factor, determined using the VIP score; and n is the number of the environmental factors considered in the HSI model. We estimated the influence of the ENSO phenomenon on habitat suitability for the greater amberjack species as well as the weighted HSI generated from the models throughout the important fishing seasons, distributed spatially.

Results

Greater amberjack time-series analysis and spatial distribution pattern of catch rates in the TS

The methodological framework of this study is presented in an overall workflow schema (Figure 1), which was used to determine how climatic events resulting from ENSO factors influence the marine environmental conditions that affect the suitable habitat of the greater amberjack in the TS. The environmental factors for the monthly time-series trend analysis from January 2014 to December 2019 are shown in Figure 2, demonstrates the strong environmental fluctuations exhibited in the TS. There is a prominent seasonal variation has been revealed between the environmental factors; from March to August (spring to summer), SST is increasing while SSS, SSH, Chl-a, and MLD are on decreasing trend. The trend pattern of EKE is more obvious opposite fluctuation shift with Chl-a, when the Chl-a is higher, EKE shows lower and vice versa throughout the year (Figure 2). The monthly average catch and catch rates of the greater amberjack in the southern and northern waters of the TS exhibited various trends (Figure 3). Similar trends were found in January, February, and March, whereas the trends varied in other months. The catch rates were higher in the northern TS than in the southern TS. Therefore, we separated the trend patterns of the southern and northern TS. Fluctuation patterns are influenced by fish availability, which is related to the environmental conditions caused by climatic events investigated in this study. The spatial distribution patterns revealed that the catch rates during spring and summer were widely distributed from 22–24°N in the

southern TS to 24–28°N in the northern TS (Figures 4A, B). In autumn, the catch rates were higher in the southern TS, with the majority of the high catch rates occurring in the southeastern waters of the TS (Figure 4C). Higher the catch rates were noted in the southern TS, from 20–24°N, throughout winter (Figure 4D).

ENSO episodes and temporal variability of catch rates of greater amberjack

The ENSO phenomenon was determined to demonstrate interannual variability in 2014–2019 (Figure 5A). The Niño Index was positive in 2015, 2016, and 2019 (El Niño years) and negative in 2017 and 2018 (La Niña years) and in 2014 (a normal year). The temporal relationship between the latitudinal gravitational center and catch rates of the greater amberjack fluctuated, demonstrating monthly and interannual variability in 2014–2019 (Figure 5B). In addition, the catch rates were higher in the El Niño periods, whereas the catch rates steadily declined in the La Niña periods. Consequently, the catch rates varied significantly ($p < 0.05$) between the ENSO episodes. The HSI model was used to analyze the impact of the ENSO phenomenon on the catch rates and habitat suitability for the greater amberjack in the TS.

Environmental variability in ENSO event periods

The oceanographic environmental characteristics, particularly the SST and SSH, in the TS changed in 2014–2019 (Figures 6A, C).
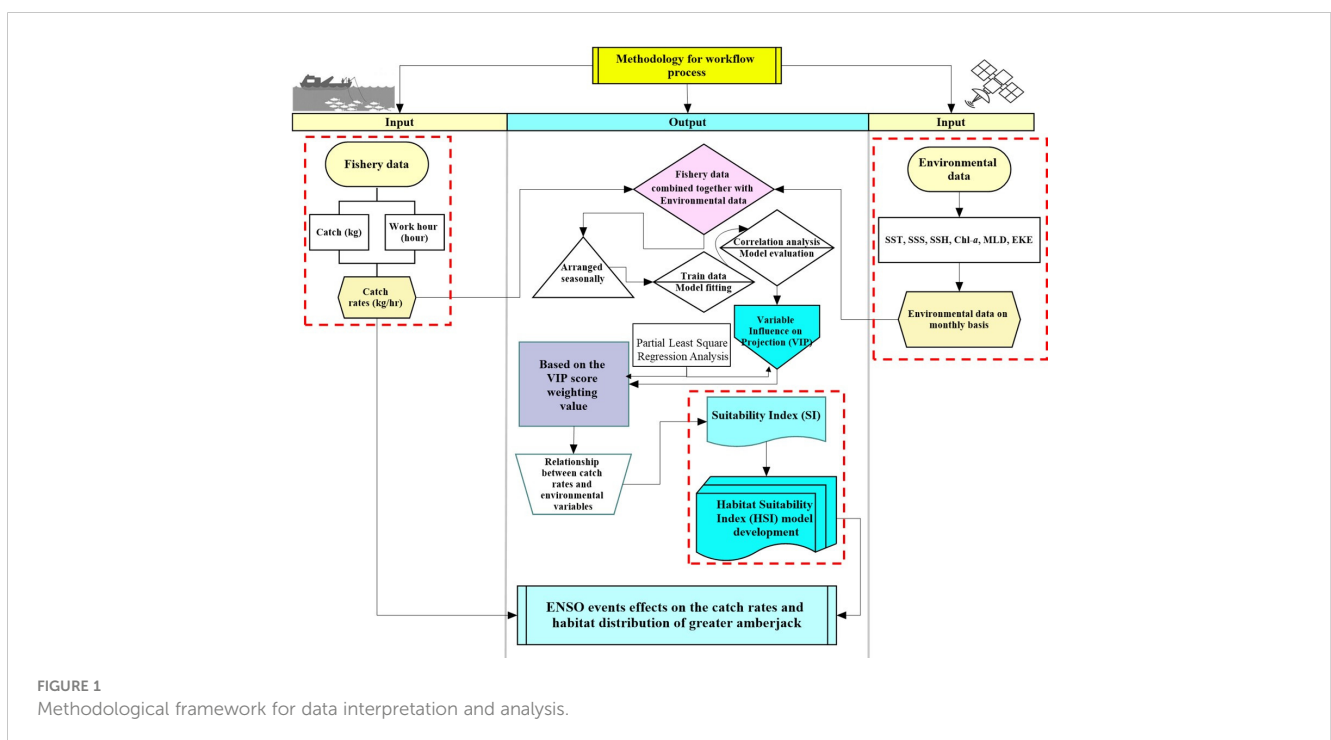

FIGURE 1
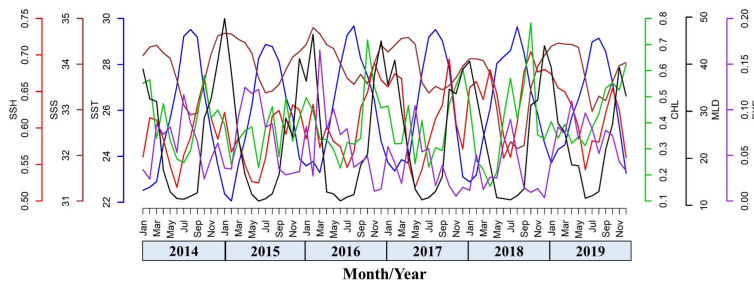Methodological framework for data interpretation and analysis.

FIGURE 2
The monthly average time series trend of environmental factors from January 2014 to December 2019 in the Taiwan Strait.
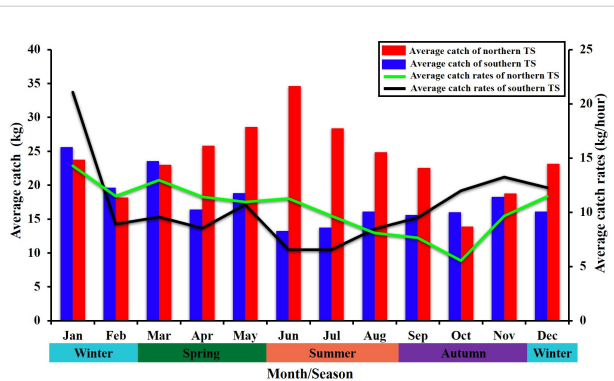

FIGURE 3
Monthly average catches and catch rates of greater amberjack in the southern and northern Taiwan Strait.

Strong positive temperature anomalies were linked with marine heatwaves in 2016 and 2019. In addition, warm anomalies were linked with El Niño periods. However, although the heatwaves caused extremely warm temperatures across the area, the warm anomalies resulting from El Niño were more spatially diverse. During the warm El Niño events, the SSS and MLD were positive anomalies, whereas during the cooler La Niña events, they were negative anomalies (Figures 6B, E). SSH variation was associated with the SST but also demonstrated a mesoscale oceanographic characteristic influence on spatiotemporal anomalies (Figure 6C). Chl-a generally exhibited an inverse relationship with the SST, exhibiting negative anomalies during warm events and positive anomalies during cool events (Figure 6D). The EKE varied substantially both spatially and temporally over the duration of the time series (Figure 6F).
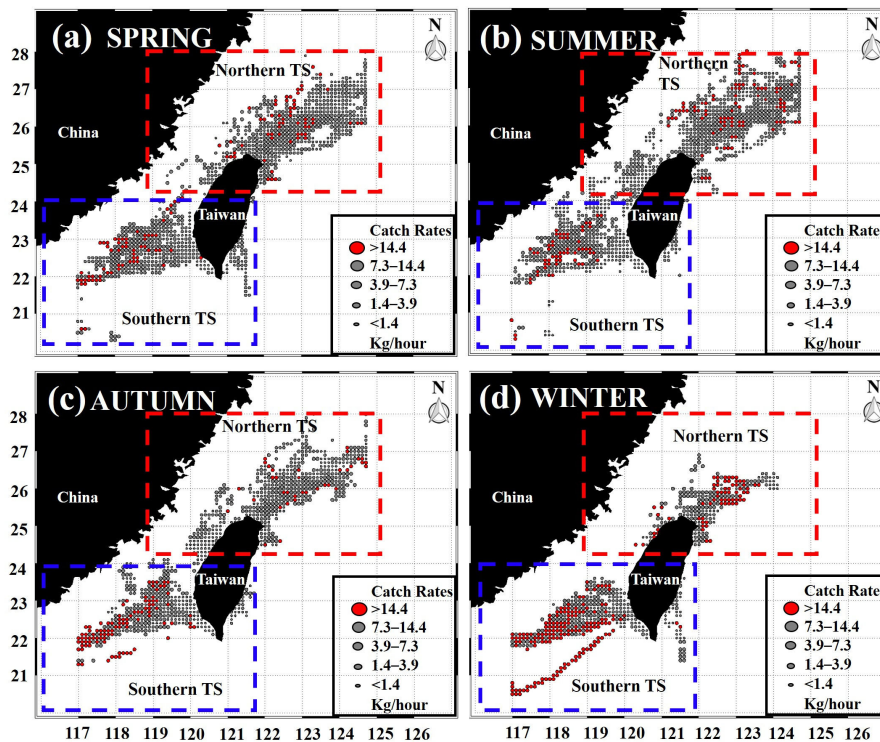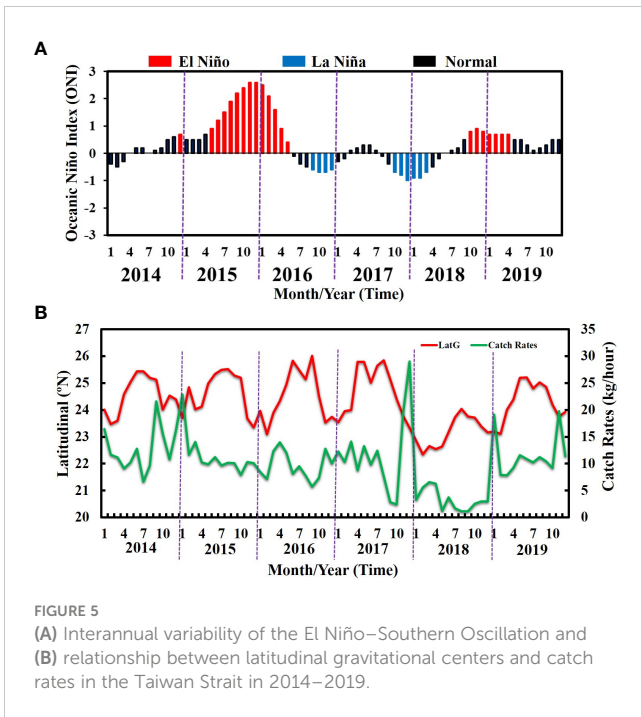

FIGURE 4
Seasonal average catch rates of greater amberjack in the southern (blue color box) and the northern (red color box) Taiwan Strait in 2014−2019.

FIGURE 5
(A) Interannual variability of the El Niño−Southern Oscillation and **(B)** relationship between latitudinal gravitational centers and catch rates in the Taiwan Strait in 2014−2019.

Association between greater amberjack catches and environmental variables in the TS

Table 1 presents the relative weighting of the key environmental variables for the greater amberjack in ENSO events, which was based on VIP scores determined using the PLSR method. In the El Niño years, the MLD and SST described the highest VIP score, and the Chl-*a* explained the lowest. In the La Niña years, the SSS described the highest VIP score, and the EKE explained the lowest. In the normal years, the MLD most described the highest VIP score,

followed by the SSH, SSS, EKE, SST, and Chl-*a* (Table 1). Box-and-whisker plots were used to demonstrate the association between the greater amberjack species and environmental variables across four seasons during ENSO events based on the fishery location data in the TS from 2014 to 2019 (Figure 7). ANOVA revealed that the greater amberjack catch rates recorded during ENSO events were significantly influenced by environmental variables throughout all seasons. The results revealed that the high catch rates in spring during El Niño events associated with a higher SST, SSS, and EKE and a lower SSH, Chl-*a*, and MLD. Low catch rates were found in the La Niña and normal years (Figures 7A1–a7). However, that there is no significant difference exhibited in the catch rates in spring between El Niño, La Niña and Normal years. The catch rates for summer were higher in the El Niño and normal years, with the catches during the two types of years demonstrating no significant differences and associated with a higher SSS and EKE and a lower SST, SSH, Chl-*a*, and MLD (Figures 7B1–b7). Moreover, the catch rates in autumn were comparable to those in summer, and higher catch rates were recorded in these seasons in the El Niño and normal years and associated with a higher SSS and EKE and a lower SSH and Chl-*a*. A higher SST was found in the El Niño years, and a higher MLD was found in the normal years (Figures 7C1–c7). In winter, higher catch rates were recorded in the El Niño and normal years and associated with a higher SSS and EKE and a lower SST, SSH, and MLD as well as a higher Chl-*a* in the normal years (Figures 7D1–d7).

Environmental variability and SI

A seasonal fitted SI model was developed for each environmental variable, and all the models was significant (*p*< 0.001), had lower root mean square differences (RMSDs), and had higher correlation coefficients (Table 2). The SI curve was used to

FIGURE 6
Hövmöller plot of anomalies in six environmental variables; **(A)** sea surface temperature anomaly (SSTA), **(B)** sea surface salinity anomaly (SSSA), **(C)** sea surface height anomaly (SSHA), **(D)** Log chlorophyll-*a* anomaly (Log Chl-*a* A), **(E)** mixed layer depth anomaly (MLDA), and **(F)** eddy kinetic energy anomaly (EKEA) during El Niño and La Niña events in the Taiwan Strait in 2014–2019.
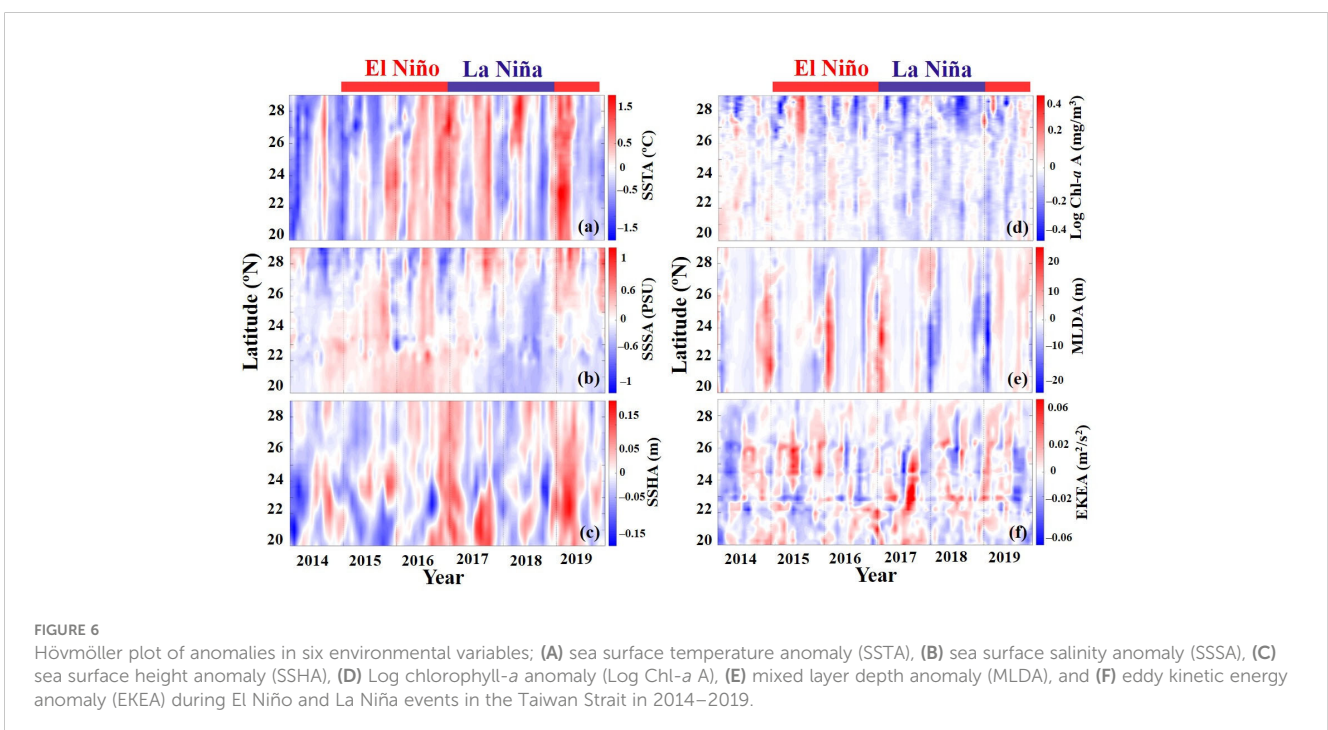
TABLE 1 Proportional weighting of the sea surface temperature (SST), sea surface salinity (SSS), sea surface height (SSH), sea surface chlorophyll-*a* (Chl-*a*), mixed layer depth (MLD), and eddy kinetic energy (EKE) in El Niño, La Niña, and normal years based on VIP scores.

Environmental variables	El Niño		La Niña		Normal	
	VIP	Importance	VIP	Importance	VIP	Importance
SST	0.32	2	0.29	2	0.06	5
SSS	0.29	3	0.37	1	0.21	3
SSH	0.18	4	0.11	5	0.26	2
Chl-*a*	0.07	6	0.12	4	0.04	6
MLD	0.44	1	0.24	3	0.26	1
EKE	0.08	5	0.10	6	0.11	4

identify various optimal ranges for all the environmental variable in each season for the greater amberjack species (Figure 8). The optimal SST ranges (SI > 0.6) were 24°C–27°C, 29°C–30°C, 27°C–29°C, and 23°C–25°C in spring, summer, autumn, and winter, respectively (Figure 8A). The SSS optimal ranges were 34.4–35 PSU in spring and winter and 33.2–34.3 PSU in summer and autumn (Figure 8B). The optimal SSH ranges in spring and summer were similar; they were 0.5–0.68 and 0.51–0.61 m, respectively. The optimal ranges in autumn and winter were 0.57–0.71 and 0.65–0.74 m, respectively (Figure 8C). The suitable Chl-*a* range was higher in summer and winter (0.13–0.32 mg/m^3) than in spring and autumn (0.12–0.18 mg/m^3; Figure 8D). Furthermore, the optimal MLD range was lower in spring and summer (9–16 m) and higher in

autumn and winter (17–28 and 28–39 m, respectively; Figure 8E). The optimal EKE range demonstrated a consistent trend across seasons (0.011–0.019 m^2/s^2; Figure 8F).

Variability in habitat suitability during ENSO events

Analysis of HSI maps revealed that the suitable habitats in spring in the El Niño and normal years were larger and extended southward (south to 23°N), whereas the suitable habitats were smaller in the La Niña years (Figures 9A–C). In summer, although the selected habitat maps indicated that the suitable
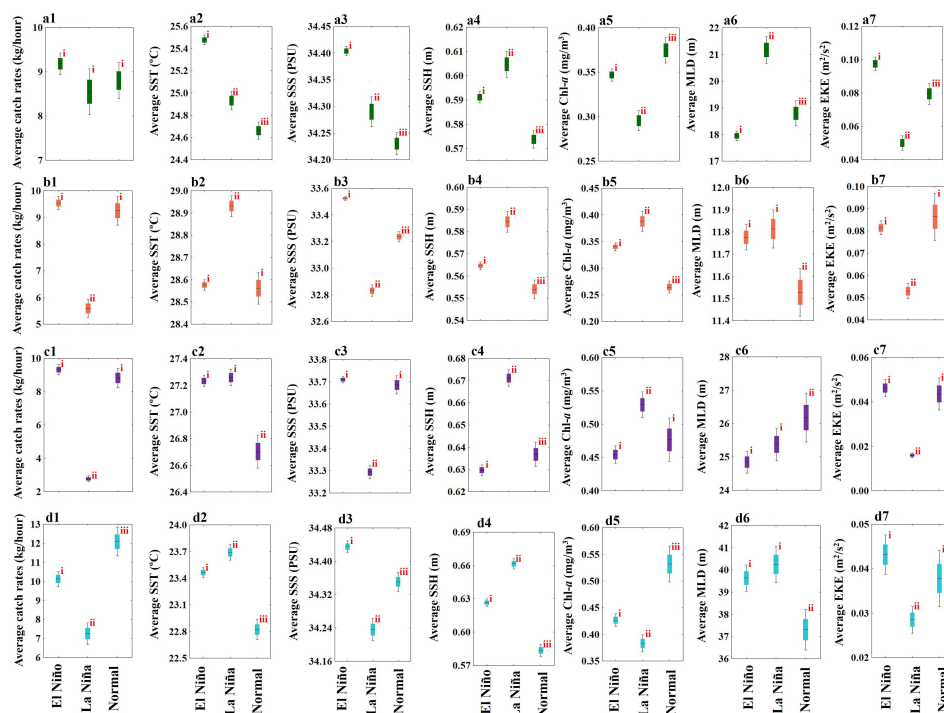

FIGURE 7
The box-and-whisker plots illustrating the effect of the environmental variables on catch rates for greater amberjack in spring **(A1–A7)**, summer **(B1–B7)**, autumn **(C1–C7)**, and winter **(D1–D7)** during ENSO events in the Taiwan Strait. The height of the box is equivalent to the standard error, and horizontal black line indicates the mean. The superscripted roman numerals denote the significant differences identified using the Tukey's test (*p* < 0.05). One-way analysis of variance was utilized to determine the significant differences of each box.

areas were larger in the southern TS (south to 22°N) during the La Niña years, the majority of the fish populations were located in the northern TS. Furthermore, in summer during the normal years, HSI values were lower, whereas in summer during the El Niño years, the catch rates and HSI values were higher, indicating that the fish populations moved further northward in the TS (Figures 9D–F). However, in autumn, the catch rates in the southern TS that matched with suitable habitats were higher in the El Niño years than in the La Niña and normal years (Figures 9G–I). The HSI maps revealed that the suitable habitats during winter in the El Niño and normal years were more northward in the northern TS and further southward in the southern TS. Furthermore, the catch rates were higher in these areas in these years than they were in the La Niña years (Figures 9J–L). The influence of ENSO events on the percentage of suitable habitats of the greater amberjack was determined to be higher in the El Niño years than in the La Niña and normal years, with different seasonal variability (Figure 10).

Spatial variability of environmental conditions and suitable habitats

The spatial habitat distribution patterns of the greater amberjack were associated with the optimal oceanographic environmental variable ranges (Table 2). The areas with variables in the optimal ranges are outlined in different colors for each season in Figures 11A–D. The habitat suitability for the greater amberjack in the TS was associated with oceanographic environmental conditions and ENSO events. Spatial correlation analysis was conducted to determine the association between HSI values and each environmental variable in the main fishing grounds between 20–28°N and 116–127°E, in the TS in 2014–2019 (Figures 12A–F). The results revealed spatial variations in the relationship between environmental conditions and habitat suitability. In the northern TS (24–28°N), the HSI value was positively correlated with the SST, SSS, SSH, and EKE, and in the southern TS (20–24°N), the value

TABLE 2 Seasonal fitted suitability index (SI) model for all the environmental variable; α and β are the estimated parameters of the SI model, and RMSD indicates the root mean square difference.

| Season	SI model	α	β	RMSD	R^2	P
Spring	SI_{SST}	−0.244	25.643	0.068	0.959	<0.001
	SI_{SSS}	−8.813	34.623	0.017	0.991	<0.001
	SI_{SSH}	−64.373	0.582	0.125	0.866	<0.001
	SI_{Chl-a}	−556.259	0.148	0.118	0.663	<0.001
	SI_{MLD}	−0.211	12.40	0.130	0.664	<0.001
	SI_{EKE}	−19532.8	0.012	0.058	0.921	<0.001
Summer	SI_{SST}	−0.728	29.146	0.074	0.920	<0.001
	SI_{SSS}	−1.572	33.713	0.052	0.960	<0.001
	SI_{SSH}	−198.57	0.558	0.056	0.962	<0.001
	SI_{Chl-a}	−229.513	0.185	0.111	0.774	<0.001
	SI_{MLD}	−2.554	10.975	0.039	0.889	<0.001
	SI_{EKE}	−14261.1	0.013	0.088	0.829	<0.001
Autumn	SI_{SST}	−0.297	27.554	0.126	0.834	<0.001
	SI_{SSS}	−2.587	33.884	0.037	0.976	<0.001
	SI_{SSH}	−94.232	0.635	0.143	0.807	<0.001
	SI_{Chl-a}	−1405.02	0.149	0.114	0.570	<0.001
	SI_{MLD}	−0.013	21.003	0.232	0.549	<0.001
	SI_{EKE}	−19423.4	0.012	0.210	0.965	<0.001
Winter	SI_{SST}	−0.272	23.955	0.086	0.921	<0.001
	SI_{SSS}	−4.941	34.593	0.027	0.983	<0.001
	SI_{SSH}	−230.132	0.686	0.144	0.740	<0.001
	SI_{Chl-a}	−160.99	0.262	0.161	0.560	<0.001
	SI_{MLD}	−0.015	33.531	0.247	0.470	<0.001
	SI_{EKE}	−22582.1	0.011	0.034	0.966	<0.001
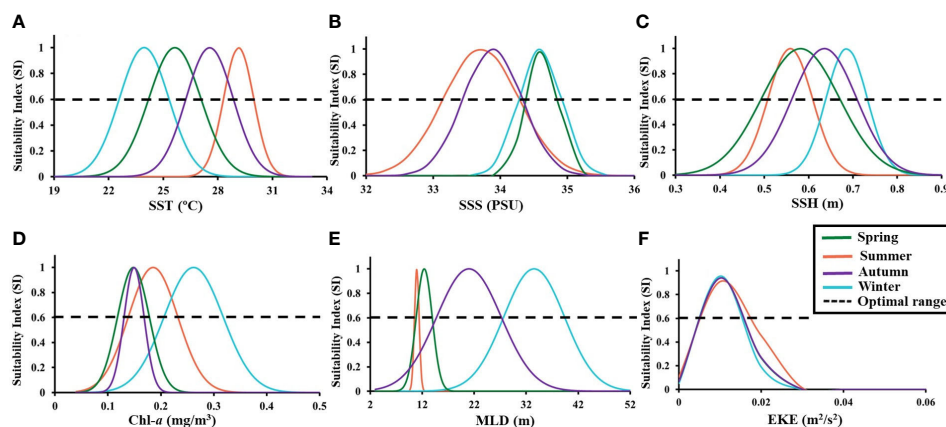
FIGURE 8
Suitability index curves fitted to the relationship between fishing effort for greater amberjack and all the environmental variable, that is, **(A)** sea surface temperature (SST), **(B)** sea surface salinity (SSS), **(C)** sea surface height (SSH), **(D)** sea surface chlorophyll-*a* (Chl-*a*), **(E)** mixed layer depth (MLD), and **(F)** eddy kinetic energy (EKE), in each season. The intersections of the SI curve and the horizontal dashed lines (SI = 0.6) are the optimal range for all the environmental variable.

was negatively correlated with the aforementioned variables, although the correlation coefficients were not high (Figures 12A–C, F). Moreover, the HSI and Chl-*a* values were significantly positively correlated in both the southern and northern TS, whereas the MLD was negatively correlated across all fishing locations (Figures 12D, E). The AMM-based HSI model results indicated significant monthly fluctuations in the HSI prediction maps. The predicted habitat shifted northward to approximately 27°N during spring and remained the same until summer. The predicted habitat then shifted southward to approximately 20–24°N in autumn and winter. The time-series latitudinal sections of the predicted HSI along the southern and northern TS revealed that the greater amberjack was primarily distributed in 20–24°N and 24–28° N. However, this area fluctuated monthly and annually (Figures 13A–F).

Discussion

Seasonal catch rate variations and spatial distribution patterns

In this study, we investigated how the oceanographic conditions resulting from ENSO events influenced the catch rates of the greater amberjack in the southern and northern TS during the study period. Moreover, we applied an AMM-based HSI modeling method to predict the habitat suitability for the greater amberjack. Our developed HSI models and analyses of the catch rates and the environmental variability may provide an insight into the climate-driven habitat suitability variations in target fish species in the TS during different ENSO events. Such research can be used to assess the effects of climate-related changes on marine environments and the quality of species-suitable habitats, which may be crucial for fishery management. Seasonal greater amberjack fishing, which was associated with various catch rates and marine environmental characteristics, was widely distributed from the southern to the

northern TS (Mammel et al., 2022). Anomalous climate events and marine environmental variability can lead to changes in catch rates and influence the spatial distribution patterns of the greater amberjack in the southern and the northern regions of the TS. According to Hasegawa et al. (2017); Hasegawa et al. (2020), the greater amberjack is a widespread species that can be found throughout the southern and northern parts of the TS.

Catches and catch rates were higher in the northern TS in spring and summer and higher in the southern TS in autumn and winter (Figure 4). This difference may be related to the selection of favorable marine habitat areas and physiological requirements of the greater amberjack. Mammel et al. (2022) reported that significant seasonal catch rate variations were strongly influenced by the marine environment, and that catches were widely distributed from north to south, indicating that the greater amberjack expanded their habitat spatial distribution range throughout the entire TS. Because all seasons are crucial for greater amberjack fisheries in the TS, we included all seasons in our study. Tone et al. (2022) used archival tag studies in northern Taiwanese waters to describe the habitat of the greater amberjack. This information can be used as a framework for analyzing changes in fish migration and spatial patterns. However, the investigation focused on the age structure and life history characteristics of the greater amberjack in the southern TS, near the thermal front region (Hasegawa et al., 2017). Although many studies have provided information on the catches and catch rates of the greater amberjack, few have been conducted in the TS.

Seasonal changes in the catch rates and marine environmental conditions of fishing grounds in the TS can be determined using remote sensing data and using daily catch data and data from vessel recorders, which are operated on Taiwanese fishing vessels. Catch rates and the variability of fish population structures are affected by climate-related oceanographic environmental conditions (Ho et al., 2016). The variability of the spatial distribution patterns of the greater amberjack may be mostly influenced by the current system in the TS. The currents in the TS, that is, the SCS, Kuroshio Branch,
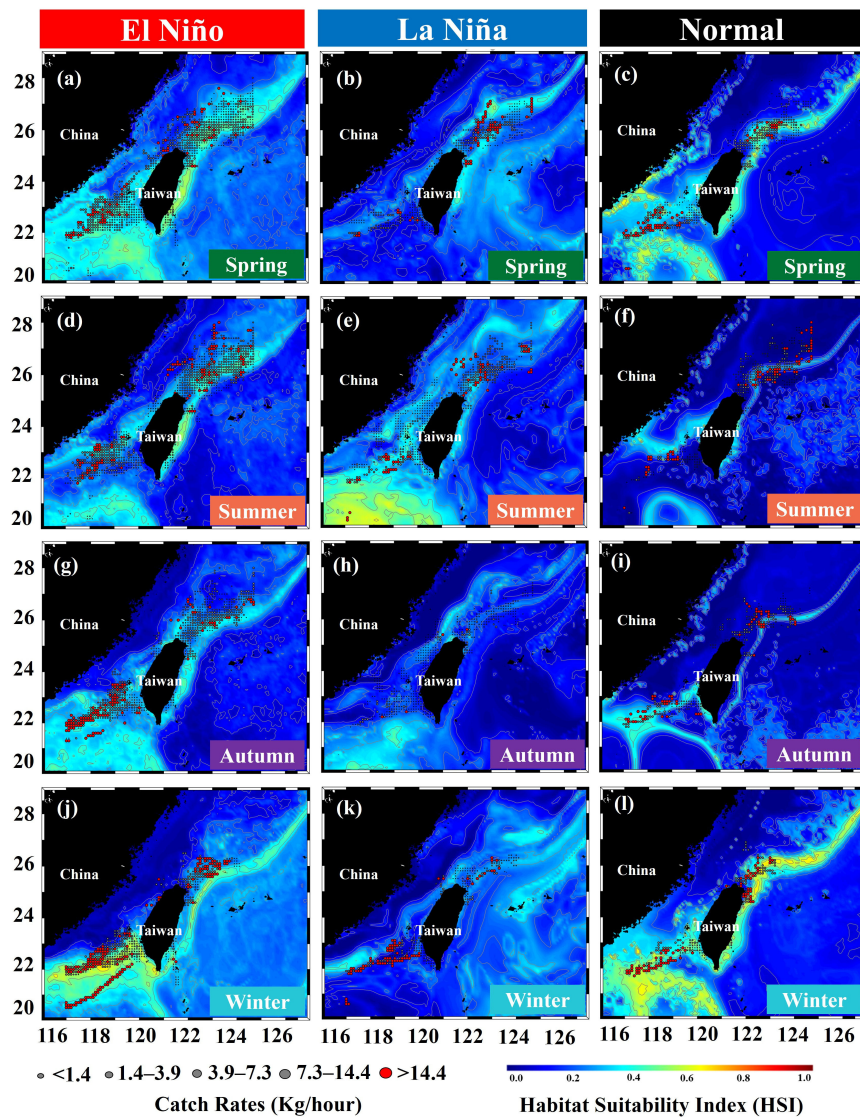
FIGURE 9
Average catch rates of greater amberjack overlaid with habitat suitability in spring **(A–C)**, summer **(D–F)**, autumn **(G–I)**, and winter **(J–L)** during ENSO events.

Kuroshio, and Coastal China Sea currents, may affect the movement of the greater amberjack in the TS when seasonal changes occur, leading to a wide distribution of the species. Previous research on various marine fish species in the TS has shown that the catch rates and spatial distribution patterns are influenced by seasonal changes in physical processes of various currents and climate-related environmental variability (Lan et al., 2014; Chen et al., 2021).

Influence of marine environmental variability on the catch rates of greater amberjack

Understanding the effects of environmental conditions on the variability of the catch rates of fish species is essential for the fisheries ecosystem-based management, which has become increasingly an accepted species management approach. However, no management or conservation strategy has been implemented for the greater amberjack in the TS, and the status of the species is unknown. Therefore, in our study, we investigated the influence of multiple dynamic environmental variables on the greater amberjack in the TS and the catch rates of the species to determine how each factor affected the species stock structure. Gaining an understanding of the association between the spatial variation of fish assemblages and marine environmental characteristics enables the habitat regions of pelagic fish to be precisely identified by using remote sensing (Brodie et al., 2015; Lee et al., 2018). A habitat is more likely to become preferable when environmental conditions are optimal. For example, the SST demonstrated considerable seasonal fluctuations, with the lowest values noted in winter (23.95°C) and highest values noted in summer (29.15°C). The SST regulates the physiological and metabolic processes of fish
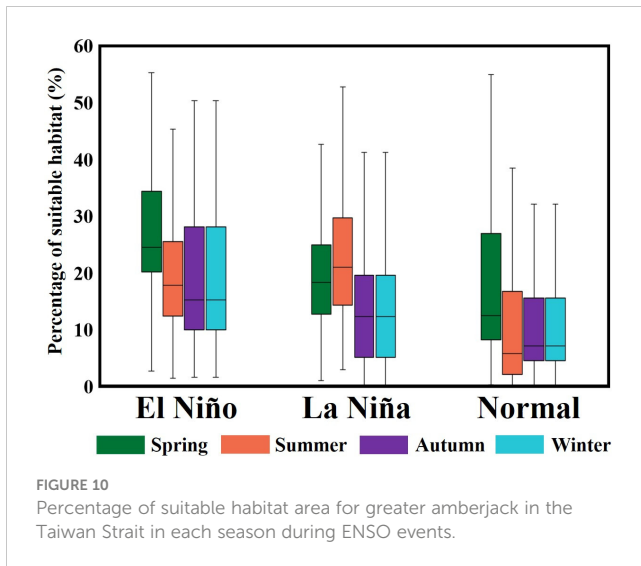
Percentage of suitable habitat area for greater amberjack in the
Taiwan Strait in each season during ENSO events.

(Abdul Azeez et al., 2021). It influences spawning, the development
of eggs and larvae, and the general distribution of fish (Gordoa et al.,
2000), and it plays a key role in the spatial distribution of marine
fish species (Hidayat et al., 2021). The SST has strong seasonal
variability in the TS and demonstrates particular variability in
summer and winter (Belkin and Lee, 2014; Lee et al., 2021).

The optimal SSS range in the fishing locations of this study was
33.2–34.3 PSU throughout summer and autumn and 34.4–35 PSU
in spring and winter. The SSS substantially influenced the habitat
quality for the greater amberjack and was higher in the El Niño
years. The SST and SSS have an inverse relationship with respect to
the seasons; a higher SST occurs when the SSS is lower (Figures 8A,
B). Salinity levels exceeding 35.8 PSU result in oligotrophic
conditions and decreased primary production, which cannot meet
the nutritional needs of pelagic fish species (Coletto et al., 2019).
The prey species aggregate near the fronts and eddies associated
with the SSH, which attracts pelagic predatory fish species (Abdul
Azeez et al., 2021). In the present study, the optimal SSH range was
lower in spring and summer (0.5–0.68 m) and higher in autumn
and winter (0.57–0.74 m) for the greater amberjack, and the SSH
value were higher in the La Niña years and lower in the El Niño
years. Mesoscale oceanographic features encourage the aggregation
of foragers by mixing nutrients and delivering them to the photic
zone, which enhances phytoplankton growth and potentially
attracts predators from higher trophic levels (Sournia, 1994).

Chl-*a* has direct and indirect associations with foraging
distribution and influences the spatial distribution of predators
(Lee et al., 2018). The optimal Chl-*a* ranges were low in spring and
autumn (0.12–0.18 mg/m^3) and high in summer and winter (0.13–
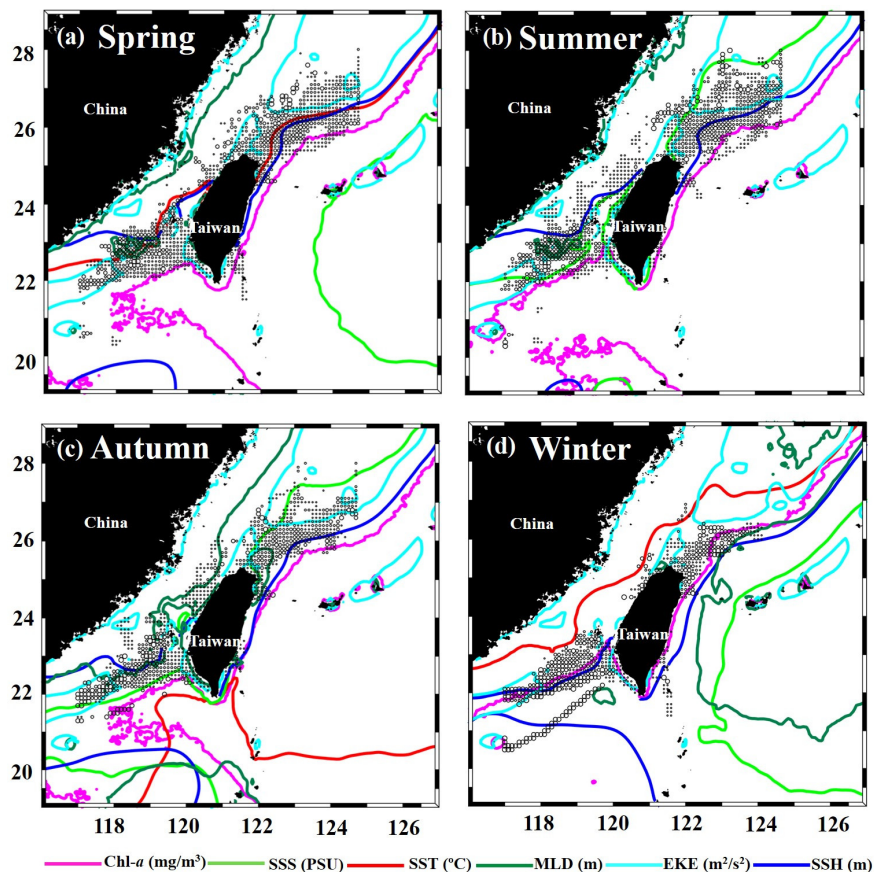0.32 mg/m^3). The summer and winter ranges may have been high

Seasonal spatial distribution of greater amberjack fisheries with most preferred environmental conditions indicated with colored lines; magenta
(Chlorophyll-*a*; Chl-*a*), light green (sea surface salinity; SSS), red (sea surface temperature; SST), dark green (mixed layer depth; MLD), aqua blue
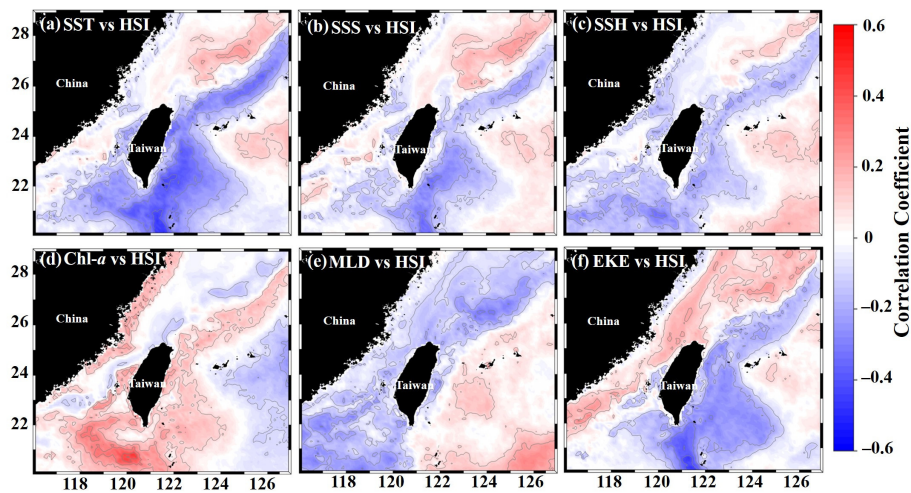(eddy kinetic energy; EKE), blue (sea surface height; SSH), respectively.

FIGURE 12
The correlation coefficients between the spatial distribution of habitat suitability index (HSI) values and environmental variables: **(A)** SST versus HSI, **(B)** SSS versus HSI, **(C)** SSH versus HSI, **(D)** Chl-a versus HSI, **(E)** MLD versus HSI, and **(F)** EKE versus HSI.

because high discharge water currents during those seasons brought nutrients to the TS. Furthermore, most fishing locations in fishery research are in coastal regions with substantial nutrient concentrations that vary with the current systems within each season in the TS. Most areas identified as potential fishing grounds are upwelling regions, which have high Chl-a and favorable SSTs, which cause sufficient nutrients to move from the layer at bottom to the top surface layer of sea waters. This often leads to high biological productivity (Hu and Wang, 2016) and influences the diet of the greater amberjack in the TS.

The MLD can serve as a proxy for SSH variation causes cooling surface temperatures can prompt to convection, which leads to an increased MLD and a decreased SSH (de Boyer Montégut et al., 2004). In the present study, we discovered that the optimal MLD range was much lower in spring and summer (9–16 m) and much higher in autumn and winter (17–39 m). Moreover, the highest catch rates for the greater amberjack in the TS were mostly found in waters with an MLD range of 10–50 m (Mammel et al., 2022). This was similar to the optimal range (11–50 m) in the western-central Gulf of Mexico (Murie et al., 2011). Seasonal changes in MLDs and
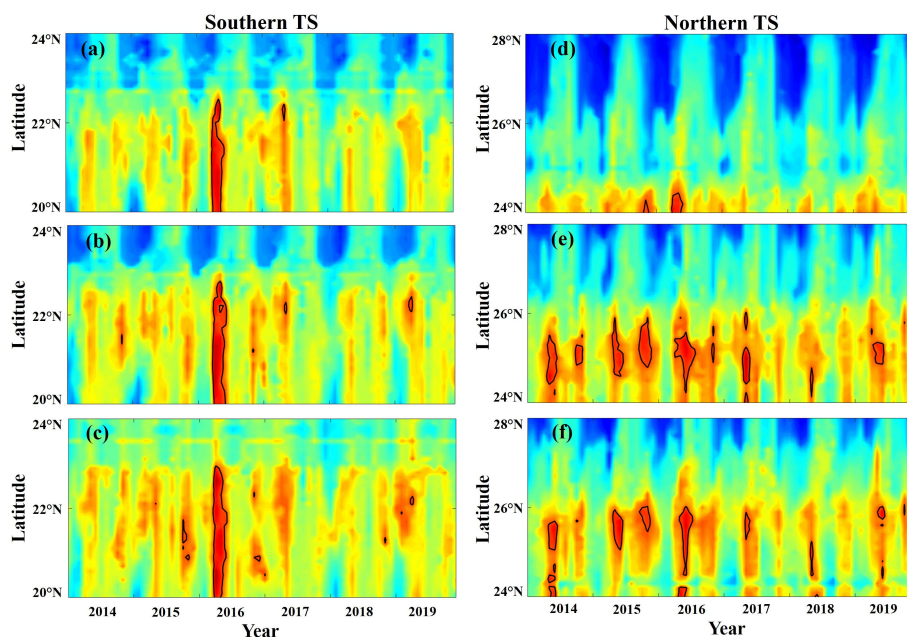

FIGURE 13
Time-series latitudinal section plots of the greater amberjack habitat suitability index (HSI) along the southern and northern Taiwan Strait: **(A)** 118°E, **(B)** 119°E, **(C)** 120°E, **(D)** 122°E, **(E)** 123°E, and **(F)** 124°E; the maps were generated using an arithmetic mean model developed using marine environmental data from 2014–2019. The black solid line outlines the areas with an HSI value of 0.8.

the transfer of water masses initiate marine environmental and biophysical mechanisms. These environmental shifts are supported by subtle biological processes, such as the distribution of nitrogen-fixing organisms (Song et al., 2022). Heat exchange and wind pressure at the seawater–air interface and turbulent mixing of the water masses play a major role in determining MLDs (Kara et al., 2003). Our findings also revealed that low EKE values have a favorable effect on greater amberjack catch rates in the TS, suggesting that an EKE higher than the optimal level can reduce the quality of suitable habitats. The optimal EKE range was 0.011–0.019 m^2/s^2 and remained similar across seasons. Studies have reported that EKE is a significant predictor of the distributions of several pelagic fish species (Champion et al., 2018; Champion et al., 2021; Mammel et al., 2022), and low EKE values have a favorable effect on the quality of kingfish (*Seriola lalandi*) habitats in Australian waters (Brodie et al., 2015; Champion et al., 2020).

ENSO events and habitat variations of greater amberjack

ENSO is a large-scale El Niño event in the tropical Pacific Ocean and is characterized by unusual SST warming, which, when together with regional environmental variability, considerably influences the fish stock dynamics of pelagic realm. No study has been conducted the impact of ENSO events on variations in the catch rates of greater amberjack fisheries in the TS. Our results indicate that the impact of ENSO on the greater amberjack catches was affected by the phase of the ENSO event. There have been many model-based approaches used to analyze habitat suitability for pelagic fish species under changing climatic conditions, and environmental variability has become a prevalent aspect of fishery research (Brodie et al., 2015; Lee et al., 2020; Mammel et al., 2022). The HSI model is among the most effective and extensively used techniques for analyzing the effects of climate variability on rapid changes in the habitat suitability for fish over time and space (Gong et al., 2011). The habitat model can be used to obtain reliable and valid information, which can then be used to understand the potential influence of anomalous environmental variability and to identify a marine species' preferred habitat.

In the present study, higher catch rates were recorded in spring, summer, and autumn in the El Niño years, with no significant differences identified between seasons. However, in winter, higher catch rates were recorded in the normal years than in the El Niño and La Niña years (Figure 7). Similarly, a study reported higher catch rates for pelagic fish species during the El Niño years in the southeast Pacific Ocean off the coastal waters of Chile (Feng et al., 2022). Despite the fact that the box-whisker plots indicate that there is no significantly difference observed in catch rates between ENSO events in spring compared to other seasons, previous research has demonstrated that the monsoon patterns had an impact on the TS during the spring, which was marked by a strong flow of the cold water China Coastal Current that carried lower temperature water and high nutrients during ENSO periods (Zhong et al., 2022). Notably, in the present study, habitat suitability during spring and summer was synchronously opposite to habitat fluctuations during ENSO events, with higher HSI values being recorded in spring in the El Niño and

normal years and higher HSI values recorded in summer in the La Niña years. This may have occurred because the greater amberjack requires higher temperature ranges (Mammel et al., 2022), and La Niña likely causes temperatures to gradually decrease in spring, which leads to the temperature being balanced in summer. This suggests that the SST was higher in summer in the La Niña years in the TS (Kuo and Ho, 2004). In the present study, in autumn, the HSI value of the southern TS was higher in the El Niño years than in the La Niña or normal years, although habitat suitability in autumn was lower than that in other seasons. Other research that employed the species distribution model revealed that the habitat suitability in the TS for the greater amberjack was less favorable in autumn (Mammel et al., 2022). Habitat suitability may be lower in autumn than in other seasons because the optimal Chl-*a* range is substantially lower in autumn (Figure 8D). This may occur because of lower nutritional supply and unfavorable environmental conditions. Our findings also revealed a higher HSI score in the southern and northern TS in winter in the El Niño and normal years. Furthermore, we discovered low HSI values in winter in the La Niña years, which did not match with the recorded catch rates. Another study reported findings that correlated well with the favorable environmental conditions in winter recorded in our study (Mammel et al., 2022); the optimal Chl-*a* and SSH ranges were comparatively higher in winter (Figures 8C, D). Furthermore, the currents and temperature increased nutrient supply and food availability for the greater amberjack in the TS.

ENSO events caused by climate variability in the Pacific Ocean are complex (Wang et al., 2017), and the effects of the events lead to changes in the habitat suitability, which may influence the fisheries (Kuczynski et al., 2018). For example, many studies have reported that commercially crucial marine species, such as large pelagic fish species (Hill et al., 2016), three swimming crab species in the TS (Naimullah et al., 2021), and jack mackerel (*Trachurus murphyi*; Feng et al., 2022), are considerably influenced by ENSO events. In this study, the latitudinal sections of the predicted HSI (Figure 13) demonstrated that the greater amberjack prefers and is highly abundant in the southern (20–24°N) and northern (24–28°N) TS, which are near to the SST frontal region (Mammel et al., 2022) and, therefore, provide favorable marine environmental conditions. This study provides preliminary findings that suggest that the catch rates and habitat suitability for the greater amberjack in the TS are related to environmental variability and ENSO. Our study only employed a habitat modeling approach to analyze the impact of ENSO events on the catch rates and habitat quality variations in different seasons, for which environmental and greater amberjack fishery data in the TS were obtained using remote sensors. Future studies should focus on SST frontal regions and spatial information related to prey dynamics. This would improve evaluations of the potential responses of the greater amberjack to environmental variability and climate change and thereby improve the understanding of suitable habitat conditions for the greater amberjack.

Conclusion

In the present study, we determined that the catch rates and habitat suitability for the greater amberjack in the TS are

considerably influenced by climate variability and marine environmental changes resulting from ENSO events in various seasons. Furthermore, global warming is causing climate change and variations in the sea temperature influence the catchability, habitat quality, and fishing pressure of fish species. High season-related habitat variability has led the greater amberjack to seek a stable and favorable environment in response to changes in climate. Our results revealed that El Niño is positively associated with higher catch rates in spring, summer, and autumn, whereas in winter, catch rates are higher in the normal years and lower in the La Niña years. During ENSO episodes, habitat suitability in spring and summer exhibits synchronized opposite variations, with higher HSI values being recorded in spring during the El Niño and normal years and in summer in the La Niña years. Habitat suitability is considerably lower in autumn than in the other seasons. In addition, the HSI value is higher in the southern and northern TS in winter in the El Niño and normal years and extremely low in winter in the La Niña years.

Our investigation is the first to elucidate the implications of climate change on the catch rates and habitat distribution of the greater amberjack in the TS. The findings of this research can be used to improve fishery management; to develop a standard harvest strategy; and to prevent time, labor, and fuel from being wasted on locating fishing grounds. Moreover, we determined the habitat of the greater amberjack was in the southern (20–24°N) and northern (24–28°N) TS. The results revealed that a high abundance of the greater amberjack and favorable oceanographic conditions are located near SST frontal areas. However, SST frontal data were not considered in this study. Future studies should consider such data and other climatic factors, such as Pacific Decadal Oscillation, that may affect habitat distribution. Future studies should also consider spatial information related to prey and apply modeling to predict habitat hotspot variability under dynamic and varying climatic and environmental conditions to enable sustainable management of the valuable species of the greater amberjack.

Data availability statement

The original contributions presented in the study are included in the article/supplementary material. Further inquiries can be directed to the corresponding author.

Author contributions

MM and M-AL conceptualized the research question and designed the study. MM and MN extracted and processed oceanographic datasets and approach with analysis of the findings from M-AL. MM wrote the manuscript. MM undertook the statistical and spatial analyses with assistance from M-AL. C-HL, Y-CW, and BS reviewed the manuscript. All authors contributed to the article and approved the submitted version.

Funding

Acknowledgments

Conflict of interest

The authors declare that the research was conducted in the absence of any commercial or financial relationships that could be construed as a potential conflict of interest.

Publisher's note

All claims expressed in this article are solely those of the authors and do not necessarily represent those of their affiliated organizations, or those of the publisher, the editors and the reviewers. Any product that may be evaluated in this article, or claim that may be made by its manufacturer, is not guaranteed or endorsed by the publisher.

References

Abdul Azeez, P., Raman, M., Rohit, P., Shenoy, L., Jaiswar, A. K., Mohammed, K., et al. (2021). Predicting potential fishing grounds of ribbonfish (*Trichiurus lepturus*) in the north-eastern Arabian Sea, using remote sensing data. *Int. J. Remote Sens.* 42, 322–342. doi: 10.1080/01431161.2020.1809025

Anderson, C. I. H., and Rodhouse, P. G. (2001). Life cycles, oceanography and variability: ommastrephid squid in variable oceanographic environments. *Fish. Res.* 54 (1), 133–143. doi: 10.1016/S0165-7836(01)00378-2

Azevedo, M., and Silva, C. (2020). A framework to investigate fishery dynamics and species size and age spatio-temporal distribution patterns based on daily resolution data: A case study using northeast Atlantic horse mackerel. *ICES J. Mar. Sci.* 77, 2933–2944. doi: 10.1093/icesjms/fsaa170

Belkin, I. M., and Lee, M. A. (2014). Long-term variability of sea surface temperature in Taiwan strait. *Clim. Change* 124, 821–834. doi: 10.1007/s10584-014-1121-4

Brodie, S., Hobday, A. J., Smith, J. A., Everett, J. D., Taylor, M. D., Gray, C. A., et al. (2015). Modelling the oceanic habitats of two pelagic species using recreational fisheries data. *Fish. Oceanogr.* 24, 463–477. doi: 10.1111/fog.12122

Carrascal, L. M., Galván, I., and Gordo, O. (2009). Partial least squares regression as an alternative to current regression methods used in ecology. *Oikos* 118, 681–690. doi: 10.1111/j.1600-0706.2008.16881.x

Champion, C., Brodie, S., and Coleman, M. A. (2021). Climate-driven range shifts are rapid yet variable among recreationally important coastal-pelagic fishes. *Front. Mar. Sci.* 8. doi: 10.3389/fmars.2021.622299

Champion, C., Hobday, A. J., Pecl, G. T., and Tracey, S. R. (2020). Oceanographic habitat suitability is positively correlated with the body condition of a coastal-pelagic fish. *Fish. Oceanogr.* 29 (1), pp.100–pp.110. doi: 10.1111/fog.12457

Champion, C., Hobday, A. J., Tracey, S. R., and Pecl, G. T. (2018). Rapid shifts in distribution and high-latitude persistence of oceanographic habitat revealed using citizen science data from a climate change hotspot. *Glob. Change Biol.* 24, 5440–5453. doi: 10.1111/gcb.14398

Chang, Y. J., Lan, K. W., Walsh, W. A., Hsu, J., and Hsieh, C. H. (2019). Modelling the impacts of environmental variation on habitat suitability for pacific saury in the northwestern pacific ocean. *Fish. Oceanogr.* 28, 291–304. doi: 10.1111/fog.12408

Chen, I. C., Hill, J. K., Ohlemüller, R., Roy, D. B., and Thomas, C. D. (2011). Rapid range shifts of species associated with high levels of climate warming. *Science* 333, 1024–1026. doi: 10.1126/science.1206432

Chen, L. C., Weng, J. S., Naimullah, M., Hsiao, P. Y., Tseng, C. T., Lan, K. W., et al. (2021). Distribution and catch rate characteristics of narrow-barred Spanish mackerel (*Scomberomorus commerson*) in relation to oceanographic factors in the waters around Taiwan. *Front. Mar. Sci.* 8, 770722. doi: 10.3389/fmars.2021.770722

Coletto, J. L., Pinho, M. P., and Madureira, L. S. P. (2019). Operational oceanography applied to skipjack tuna (*Katsuwonus pelamis*) habitat monitoring and fishing in south-western Atlantic. *Fish. Oceanogr.* 28, 82–93. doi: 10.1111/fog.12388

de Boyer Montégut, C., Madec, G., Fischer, A. S., Lazar, A., and Iudicone, D. (2004). Mixed layer depth over the global ocean: An examination of profile data and a profile-based climatology. *J. Geophys. Res. Oceans* 109, 1–20. doi: 10.1029/2004JC002378

Feng, Z., Yu, W., and Chen, X. (2022). Concurrent habitat fluctuations of two economically important marine species in the southeast pacific ocean off Chile in relation to ENSO perturbations. *Fish. Oceanogr.* 31, 123–134. doi: 10.1111/fog.12566

Garrison, L. P., Michaels, W., Link, J. S., and Fogarty, M. J. (2002). Spatial distribution and overlap between ichthyoplankton and pelagic fish and squids on the southern flank of georges bank. *Fish. Oceanogr.* 11, 267–285. doi: 10.1046/j.1365-2419.2002.00205.x

Gold, J. R., and Richardson, L. R. (1998). Population structure in greater amberjack, *Seriola dumerili*, from the gulf of Mexico and the western Atlantic ocean. *Fish. Bull.* 96, 767–778.

Gong, C. X., Chen, X. J., Gao, F., Guan, W. J., and Lei, L. (2011). Review on habitat suitability index in fishery science. *J. Ocean Univ. China* 20 (2), 260–269.

Gong, G. C., Wen, Y. H., Wang, B. W., and Liu, G. J. (2003). Seasonal variation of chlorophyll a concentration, primary production and environmental conditions in the subtropical East China Sea. *Deep Sea Res. Part II Top. Stud. Oceanogr.* 50, 1219–1236. doi: 10.1016/S0967-0645(03)00019-5

Gordoa, A., Maso, M., and Voges, L. (2000). ""Satellites and fisheries: The Namibian hake, a case study."," in *Satellites, oceanography and society*. Ed. D. Halpern (Amsterdam: Elsevier), 193–205.

Hasegawa, T., Lu, C. P., Hsiao, S. T., Uchino, T., Yeh, H. M., Chiang, W. C., et al. (2020). Distribution and genetic variability of young-of-the-year greater amberjack (*Seriola dumerili*) in the East China Sea. *Environ. Biol. Fishes* 103, 833–846. doi: 10.1007/s10641-020-00985-6

Hasegawa, T., Yeh, H. M., Chen, J. R., Kuo, C. L., Kawabe, R., and Sakakura, Y. (2017). Collection and aging of greater amberjack *Seriola dumerili* larvae and juveniles around the penghu islands, Taiwan. *Ichthyol. Res.* 64, 145–150. doi: 10.1007/s10228-016-0543-6

Hidayat, R., Zainuddin, M., Mallawa, A., Mustapha, M. A., and Putri, A. R. S. (2021). Mapping spatial-temporal skipjack tuna habitat as a reference for fish aggregating devices (Fads) settings in makassar strait, Indonesia. *Biodiversitas J. Biol. Diversity* 22, 3637–3647. doi: 10.13057/biodiv/d220905

Hill, N. J., Tobin, A. J., Reside, A. E., Pepperell, J. G., and Bridge, T. C. (2016). Dynamic habitat suitability modelling reveals rapid poleward distribution shift in a mobile apex predator. *Glob. Change Biol.* 22, 1086–1096. doi: 10.1111/gcb.13129

Ho, C. H., Lu, H. J., He, J. S., Lan, K. W., and Chen, J. L. (2016). Changes in patterns of seasonality shown by migratory fish under global warming: Evidence from catch data of taiwan's coastal fisheries. *Sustainability* 8 (3), 273. doi: 10.3390/su8030273

Hu, J., and Wang, X. H. (2016). Progress on upwelling studies in the China seas. *Rev. Geophys.* 54, 653–673. doi: 10.1002/2015rg000505

Kai, M., Thorson, J. T., Piner, K. R., and Maunder, M. N. (2017). Predicting the spatio-temporal distributions of pelagic sharks in the western and central north pacific. *Fish. Oceanogr.* 26, 569–582. doi: 10.1111/fog.12217

Kara, A. B., Rochford, P. A., and Hurlburt, H. E. (2003). Mixed layer depth variability over the global ocean. *J. Geophys. Res. Oceans* 108 (C3), 3079. doi: 10.1029/2000jc000736

Kuczynski, L., Legendre, P., and Grenouillet, G. (2018). Concomitant impacts of climate change, fragmentation and non-native species have led to reorganization of fish communities since the 1980s. *Glob. Ecol. Biogeogr.* 27, 213–222. doi: 10.1111/geb.12690

Kuo, N. J., and Ho, C. R. (2004). ENSO effect on the sea surface wind and sea surface temperature in the Taiwan strait. *Geophys. Res. Lett.* 31 (13), L13311. doi: 10.1029/2004GL020303

Lan, K. W., Kawamura, H., Lee, M. A., Chang, Y., Chan, J. W., and Liao, C. H. (2009). Summertime sea surface temperature fronts associated with upwelling around the Taiwan bank. *Cont. Shelf Res.* 29, 903–910. doi: 10.1016/j.csr.2009.01.015

Lan, K. W., Lee, M. A., Zhang, C. I., Wang, P. Y., Wu, L. J., and Lee, K. T. (2014). Effects of climate variability and climate change on the fishing conditions for grey

mullet (*Mugil cephalus* l.) in the Taiwan strait. *Clim. Change* 126, pp.189–pp.202. doi: 10.1007/s10584-014-1208-y

Lan, K. W., Lian, L. J., Li, C. H., Hsiao, P. Y., and Cheng, S. Y. (2020). Validation of a primary production algorithm of vertically generalized production model derived from multi-satellite data around the waters of Taiwan. *Remote Sens.* 12 (10), 1627. doi: 10.3390/rs12101627

Lee, M. A., Huang, W. P., Shen, Y., Weng, J. S., Semedi, B., Wang, Y. C., et al. (2021). Long-term observations of interannual and decadal variation of sea surface temperature in the Taiwan strait. *J. Mar. Sci. Tech-Taiw.* 29, 525–536. doi: 10.51400/2709-6998.1587

Lee, D., Son, S. H., Kim, W., Park, J. M., Joo, H., and Lee, S. H. (2018). Spatio-temporal variability of the habitat suitability index for chub mackerel (*Scomber japonicus*) in the East/Japan Sea and the south Sea of south Korea. *Remote Sens.* 10 (6), 938. doi: 10.3390/rs10060938

Lee, M. A., Weng, J. S., Lan, K. W., Vayghan, A. H., Wang, Y. C., and Chan, J. W. (2020). Empirical habitat suitability model for immature albacore tuna in the north pacific ocean obtained using multisatellite remote sensing data. *I. J. Remote Sens.* 41, 5819–5837. doi: 10.1080/01431161.2019.1666317

Lee, M. A., Yeah, C. D., Cheng, C. H., Chan, J. W., and Lee, K. T. (2003). Empirical orthogonal function analysis of AVHRR sea surface temperature patterns in Taiwan strait. *J. Mar. Sci. Tech-Taiw.* 11, 1–7. doi: 10.51400/2709-6998.2269

Li, G., Chen, X., Lei, L., and Guan, W. (2014). Distribution of hotspots of chub mackerel based on remote-sensing data in coastal waters of China. *I. J. Remote Sens.* 35, 4399–4421. doi: 10.1080/01431161.2014.916057

Mammel, M., Naimullah, M., Vayghan, A. H., Hsu, J., Lee, M.-A., Wu, J.-H., et al. (2022). Variability in the spatiotemporal distribution patterns of greater amberjack in response to environmental factors in the Taiwan strait using remote sensing data. *Remote Sens.* 14, 2932. doi: 10.3390/rs14122932

Mansor, S., Tan, C. K., Ibrahim, H. M., and Shariff, A. R. M. (2001). "Satellite fish forecasting in south China sea," In *Proceedings of the 22nd Asian Conference on Remote Sensing,* Singapore, Vol. 5.

McPhaden, M. J., Zebiak, S. E., and Glantz, M. H. (2006). ENSO as an integrating concept in earth science. *Science* 314, 1740–1745. doi: 10.1126/science.1132588

Murie, D., Parkyn, D., and Austin, J. (2011). "Seasonal movement and mixing rates of greater amberjack in the gulf of Mexico and assessment of exchange with the south Atlantic spawning stock," in *Southeast data, assessment and review; 33-DW12* (North Charleston, SC, USA: SEDAR).

Naik, H., and Chen, C. T. (2008). Biogeochemical cycling in the Taiwan strait. *Estuar. Coast. Shelf Sci.* 78, 603–612. doi: 10.1016/j.ecss.2008.02.004

Naimullah, M., Lan, K. W., Liao, C. H., Hsiao, P. Y., Liang, Y. R., and Chiu, T. C. (2020). Association of environmental factors in the Taiwan strait with distributions and habitat characteristics of three swimming crabs. *Remote Sens.* 12 (14), 2231. doi: 10.3390/rs12142231

Naimullah, M., Wu, Y. L., Lee, M. A., and Lan, K. W. (2021). Effect of the El niño–southern oscillation (ENSO) cycle on the catches and habitat patterns of three swimming crabs in the Taiwan strait. *Front. Mar. Sci.* 8. doi: 10.3389/fmars.2021.763543

Nakada, M. (2008). "Capture-based aquaculture of yellowtail," in *Capture-based aquaculture: global overview*. Eds. A. Lovatelli and P. F. Holthus (Rome: FAO Fisheries Technical Paper), p 199–p 215.

Pecl, G., Araujo, M., Bell, J., Blanchard, J., Bonebrake, T., Chen, I., et al. (2017). Biodiversity redistribution under climate change: impacts on ecosystems and human wellbeing. *Science* 355 (6332), eaai9214. doi: 10.1126/SCIENCE.AAI9214

Poloczanska, E. S., Brown, C. J., Sydeman, W. J., Kiessling, W., Schoeman, D. S., Moore, P. J., et al. (2013). Global imprint of climate change on marine life. *Nat. Clim. Change* 3, 919–925. doi: 10.1038/nclimate1958

Saraux, C., Fromentin, J. M., Bigot, J. L., Bourdeix, J. H., Morfin, M., Roos, D., et al. (2014). Spatial structure and distribution of small pelagic fish in the northwestern mediterranean sea. *PloS One* 9 (11), e111211. doi: 10.1371/journal.pone.0111211

Sassa, C., and Tsukamoto, Y. (2010). Distribution and growth of *Scomber japonicus* and *S. australasicus* larvae in the southern East China Sea in response to oceanographic conditions. *Mar. Ecol. Prog. Ser.* 419, 185–199. doi: 10.3354/meps08832

Sassa, C., Tsukamoto, Y., Nishiuchi, K., and Konishi, Y. (2008). Spawning ground and larval transport processes of jack mackerel *Trachurus japonicus* in the shelf-break region of the southern East China Sea. *Cont. Shelf Res.* 28, 2574–2583. doi: 10.1016/j.csr.2008.08.002

Silva, C., Andrade, I., Yáñez, E., Hormazabal, S., Barbieri, M.Á., Aranis, A., et al. (2016). Predicting habitat suitability and geographic distribution of anchovy (*Engraulis ringens*) due to climate change in the coastal areas off Chile. *Prog. Oceanogr.* 146, 159–174. doi: 10.1016/j.pocean.2016.06.006

Sley, A., Taieb, A. H., Jarboui, O., Ghorbel, M., and Bouain, A. (2016). Feeding behaviour of greater amberjack *Seriola dumerili* (Risso 1810) from central Mediterranean (Gulf of gabes, Tunisia). *J. Mar. Biolog. Assoc.* 96, 1229–1234. doi: 10.1017/S0025315415001770

Song, Y., Wang, C., and Sun, D. (2022). Both dissolved oxygen and chlorophyll explain the Large-scale longitudinal variation of deep scattering layers in the tropical pacific ocean. *Front. Mar. Sci.* 9. doi: 10.3389/fmars.2022.782032

Sournia, A. (1994). Pelagic biogeography and fronts. *Prog. Oceanogr.* 34, 109–120. doi: 10.1016/0079-6611(94)90004-3

Taki, Y., Kohno, H., Sakamaot, K., and Hosoya, K. (2005). *Illustrated fishes in colour revised edition* (Tokyo: Hokuryukan Co. Ltd.).

Tanaka, K., and Chen, Y. (2016). Modeling spatiotemporal variability of the bioclimate envelope of *Homarus americanus* in the coastal waters of Maine and new Hampshire. *Fish. Res.* 177, 137–152. doi: 10.1016/j.fishres.2016.01.010

Tian, Y., Akamine, T., and Suda, M. (2003). Variations in the abundance of pacific saury (*Cololabis saira*) from the northwestern pacific in relation to oceanic-climate changes. *Fish. Res.* 60, 439–454. doi: 10.1016/S0165-7836(02)00143-1

Tone, K., Nakamura, Y., Chiang, W. C., Yeh, H. M., Hsiao, S. T., Li, C. H., et al. (2022). Migration and spawning behavior of the greater amberjack *Seriola dumerili* in eastern Taiwan. *Fish. Oceanogr.* 31, 1–18. doi: 10.1111/fog.12559

Tseng, H. C., You, W. L., Huang, W., Chung, C. C., Tsai, A. Y., Chen, T. Y., et al. (2020). Seasonal variations of marine environment and primary production in the Taiwan strait. *Front. Mar. Sci.* 7. doi: 10.3389/fmars.2020.00038

Turner, S. C., Cummings, N. J., and Porch, C. E. (2000). *Stock assessments of gulf of Mexico greater amberjack using data through 1998. southeast data, assessment and review, S9RD06*; SEDAR: North Charleston, SC, USA.

Vayghan, A. H., Lee, M. A., Weng, J. S., Mondal, S., Lin, C. T., and Wang, Y. C. (2020). Multisatellite-based feeding habitat suitability modeling of albacore tuna in the southern Atlantic ocean. *Remote Sens.* 12 (16), 2515. doi: 10.3390/RS12162515

Wang, C., Deser, C., Yu, J. Y., DiNezio, P., and Clement, A. (2017). *El Niño and southern oscillation (ENSO): a review. coral reefs of the Eastern tropical pacific* (Dordrecht: Springer), 85–106. doi: 10.1007/978-94-017-7499-4_4

Ward, E. J., Jannot, J. E., Lee, Y.-W., Ono, K., Shelton, A. O., and Thorson, J. T. (2015). Using spatiotemporal species distribution models to identify temporally evolving hotspots of species co-occurrence. *Ecol. Appl.* 25, 2198–2209. doi: 10.1890/15-0051.1

Wold, S., Sjöström, M., and Eriksson, L. (2001). PLS-regression: a basic tool of chemometrics. *Chemometr. Intell. Lab. Syst.* 58, 109–130. doi: 10.1016/s0169-7439(01)00155-1

Wu, L., Cai, W., Zhang, L., Nakamura, H., Timmermann, A., Joyce, T., et al. (2012). Enhanced warming over the global subtropical western boundary currents. *Nat. Clim. Change* 2, 161–166. doi: 10.1038/nclimate1353

Yen, K. W., Lu, H. J., Chang, Y., and Lee, M. A. (2012). Using remote-sensing data to detect habitat suitability for yellowfin tuna in the Western and central pacific ocean. *I. J. Remote Sens.* 33, 7507–7522. doi: 10.1080/01431161.2012.685973

Yu, W., and Chen, X. (2020). Habitat suitability response to sea-level height changes: Implications for ommastrephid squid conservation and management. *Aqua. Fish.* 6 (3), 309–320. doi: 10.1016/j.aaf.2020.06.001

Zhang, X., Saitoh, S. I., and Hirawake, T. (2017). Predicting potential fishing zones of Japanese common squid (*Todarodes pacificus*) using remotely sensed images in coastal waters of south-western Hokkaido, Japan. *I. J. Remote Sens.* 38, 6129–6146. doi: 10.1080/01431161.2016.1266114

Zhong, Y., Laws, E. A., Zhuang, J., Wang, J., Wang, P., Zhang, C., et al. (2022). Responses of phytoplankton communities driven by differences of source water intrusions in the El niño and la niña events in the Taiwan strait during the early spring. *Front. Mar. Sci.* 9, 997591. doi: 10.3389/fmars.2022.997591